Amino-Terminally Truncated Aβ Peptide Species Are the Main Component of Cotton Wool Plaques[†]

Leticia Miravalle,[‡] Miguel Calero,[§] Masaki Takao,[‡] Alex E. Roher,[||] Bernardino Ghetti,[‡] and Ruben Vidal*[,‡]

Indiana Alzheimer Disease Center, Department of Pathology and Laboratory Medicine, Indiana University School of Medicine, Indianapolis, Indiana 46202, Centro Nacional de Microbiología, Majadahonda-Madrid 28220, Spain, and Longtine Center for Molecular Biology and Genetics, Sun Health Research Institute, Sun City, Arizona 85351

Received May 4, 2005; Revised Manuscript Received June 15, 2005

ABSTRACT: Cotton wool plaques (CWPs) are round lesions that lack a central amyloid core. CWPs have been observed in individuals affected by early-onset familial Alzheimer disease (FAD) associated with mutations in the presenilin 1 (*PSEN1*) gene. Here we present the characterization of the amyloid-β (Aβ) peptides deposited in the brain of an individual affected by FAD carrying the novel missense (V261I) mutation in the *PSEN1* gene. Matrix-assisted laser desorption ionization time-of-flight mass spectrometry was used to determine the Aβ peptide species present in the cerebral and cerebellar cortices, in leptomeningeal vessels, and in CWPs isolated by laser microdissection (LMD). Our results indicate that amino-terminally truncated Aβ peptide species ending at residues 42 and 43 are the main Aβ peptides deposited in brain parenchyma and LMD-CWPs in association with the *PSEN1* V261I mutation. Full-length Aβ1−42 and Aβ1−43 peptide species were underrepresented. CWPs were not found to be associated with vessels and did not contain Aβ1−40 peptides, the main component of the vascular deposits. Although Aβ deposits were present mostly in the form of CWPs in the cerebral cortex and as diffuse deposits in the cerebellar cortex, a similar array of amino-terminally truncated Aβ peptide species was seen in both cases. The biochemical data support the concept that parenchymal and vascular amyloid deposits are associated with a different array of Aβ peptide species. The generation and parenchymal deposition of highly insoluble amino-terminally truncated Aβ peptides may play an important role in the pathogenesis of AD and must be taken into consideration in developing new diagnostic and therapeutic strategies.

A hallmark of Alzheimer disease (AD)[1] pathology is the accumulation in brain parenchyma and in vessel walls of the insoluble 4 kDa amyloid-β (Aβ) peptide (*1*). Aβ is generated by the proteolysis of the amyloid-β precursor protein (AβPP) by the β-site AβPP-cleaving enzyme 1 (BACE1) (*2*) and by γ-secretase, a multimeric protein complex composed of presenilin, nicastrin, Aph-1, and Pen-2 (*3*). After cleavage of AβPP at the amino terminus of the Aβ domain by BACE1, cleavage of the carboxyl-terminal fragment (CTF) of AβPP results in the release of the Aβ peptide (*1*−*3*). Amyloid deposits in human brain contain Aβ peptides of 40 (Aβ1−40) or 42 (Aβ1−42) amino acids in length but also various species of amino- and carboxyl-truncated Aβ peptides (*1*). Aβ1−42 forms fibrils significantly faster and is more neurotoxic than Aβ1−40 (*4*, *5*). Thus, the fibrillization of Aβ1−42 into amyloid deposits has been considered a key element in the pathogenesis of AD (*1*). Interestingly, recent studies have demonstrated that oligomeric nonfibrillar Aβ1−42 peptides and protofibrils are also neurotoxic (*6*, *7*).

In the brain parenchyma, Aβ peptides are the main component of senile plaques and diffuse deposits. Senile plaques contain a heterogeneous mixture of Aβ peptide species comprising Aβ1−42, amino-terminally modified and truncated Aβ peptides ending at positions 42 and 43, and posttranslationally modified Aβ peptides (*8*−*13*). The relative importance of amino-terminally truncated and posttranslationally modified Aβ peptides in the pathogenesis of AD is still not completely understood (*14*, *15*). Amino-terminally truncated Aβ peptide species have been found in individuals with sporadic AD, familial AD (FAD), and Down syndrome (DS) (*10*, *12*, *13*, *15*−*17*), as well as in cell cultures (*18*). Diffuse deposits, which are mostly found in the cerebral and cerebellar cortices, neostriatum, and hypothalamus, have been shown to contain the amino-terminally truncated Aβ17−42 peptide (p3) originated by the cleavage of AβPP by α-secretase and γ-secretase (*19*, *20*). Diffuse deposits also contain full-length Aβ1−42 and Aβ1−43 [Aβ1−42(43)] and amino-terminally modified and truncated Aβ peptides ending at positions 42 and 43 (*17*). In the vascular compartment, Aβ deposition is found in the walls of large and small leptomeningeal vessels as well as intraparenchymal medium-sized

[†] This work was supported by Grants P30 AG10133 and R01 AG019795, the Alzheimer's Association, AFAR, and Red CIEN (C03/06).

* Corresponding author. Phone: (317) 274-1729. Fax: (317) 274-0504. E-mail: rvidal@iupui.edu.

[‡] Indiana University School of Medicine.

[§] Centro Nacional de Microbiología.

[||] Sun Health Research Institute.

[1] Abbreviations: Aβ, amyloid-β peptide; AβPP, amyloid-β precursor protein; AD, Alzheimer disease; BACE, β-site AβPP-cleaving enzyme; CAA, cerebral amyloid angiopathy; CWP, cotton wool plaque; DS, Down syndrome; FAD, familial Alzheimer disease; MALDI-TOF-MS, matrix-assisted laser desorption ionization time-of-flight mass spectrometry; PSEN1, presenilin 1.

10.1021/bi0508237 CCC: $30.25
Published on Web 07/22/2005

and small vessels. Aβ1−40 is the predominant form present in the amyloid deposits, with carboxyl-terminal truncated derivatives found in both leptomeningeal and cortical vessels (*10*, *21*, *22*).

Herein, we present our studies using matrix-assisted laser desorption ionization time-of-flight mass spectrometry (MALDI-TOF-MS) to determine the Aβ peptide species present in frontal cortex and cerebellum of a FAD-affected individual carrier of the novel *PSEN1* V261I mutation. MALDI-TOF-MS was also used to establish the Aβ peptide species present in laser microdissected (LMD) CWPs from carriers of the *PSEN1* V261I and *PSEN1* V261F mutations. The biochemical and pathological data clearly demonstrate that there is a differential contribution of amyloid peptides of different lengths to the development of the parenchymal and vascular amyloid pathology associated with the *PSEN1* V261I mutation. Amino-terminally truncated Aβ peptide species with and without a pyroglutamyl residue at positions Glu-3 and Glu-11, and ending at positions 42 and 43, were seen as the main Aβ peptide species present in LMD-CWPs. The finding of a similar array of amino-terminally truncated Aβ peptide species in the cerebral cortex (mostly deposited as CWPs) and in the cerebellar cortex (forming diffuse deposits) strongly suggests that tissue-specific factors may play an important role in determining the morphology of the Aβ deposits. Our data suggest that the generation and deposition of Aβ peptides of different lengths may constitute the basis for the morphological diversity seen in association with early-onset FAD. Our data also support the concept that amino-terminally truncated Aβ peptides may have an important role in the pathogenesis of AD and should be taken into consideration in developing new diagnostic and therapeutic strategies.

EXPERIMENTAL PROCEDURES

Antibodies. Several antibodies (the epitope recognized by the antibody is indicated between parentheses) were used to analyze the amino-terminal sequence of the Aβ peptide. These included monoclonal 3D6 (Aβ1−5) (*23*) (Elan Corp., San Francisco, CA), monoclonal 10D5 (Aβ3−6) (*24*) (Elan Corp.), polyclonal anti-Aβ with a pyroglutamyl residue at the amino-terminal position Glu-3 (AβN3pE) (*16*) (IBL Co., Gunma, Japan), and monoclonal 6E10 (Aβ3−8) (Signet Laboratories, Dedham, MA). Monoclonal HYB310-01 (Aβ10−16) (Antibody Shop, Copenhagen, Denmark) and monoclonal 4G8 (Aβ18−22) (Signet) were used to detect full-length Aβ and Aβ species originated by the α-secretase cleavage between amino acids 16 and 17 of the Aβ sequence (p3), respectively. Aβ species ending at residue 40 (AβN−40) were recognized using polyclonal anti-AβN−40 (*25*). Aβ species ending at residue 42 (AβN−42) were recognized using monoclonal 21F12 (Elan Corp.). We also used monoclonal F8/86 (anti-von Willebrand factor or factor VIII) (Dako, Carpinteria, CA), monoclonal 3D12 (anti-apolipoprotein E) (Accurate, Westbury, NY), monoclonal AT8 (antiphosphorylated tau at Ser202/Thr205) (Polymedco, Inc.), monoclonal 1A4 (anti-alpha smooth muscle actin or αSMA) (Dako), and polyclonal anti-α-synuclein (raised against amino acids 119−137 of α-synuclein) (*22*).

Genetic Analysis. Genomic DNA was extracted from frozen brain tissue. Polymerase chain reaction (PCR) was performed for the amplification of the *PSEN1* and *AβPP* genes as described (*22*, *26*). PCR products were sequenced on a CEQ 2000XL DNA analysis system (Beckman Coulter, Fullerton, CA). Apolipoprotein E genotyping was performed as described (*22*).

Neurohistology and Immunohistochemistry. A brain autopsy was carried out on an individual carrying the *PSEN1* V261I mutation. The fresh brain was hemisected along the midsagittal plane; the right half of the brain was fixed in 10% formalin, and the left half was sliced and stored at −70 °C. The neuropathological study was carried out using techniques previously described (*26*). Eight micrometer thick sections were stained with the hematoxylin−eosin (H&E) and Bodian methods. Congo red stain and thioflavin S (Th-S) were used to show the presence of amyloid deposits and neurofibrillary tangles. For immunohistological studies, antibodies against Aβ, phosphorylated tau, α-synuclein, apolipoprotein E, factor VIII, and αSMA were used. Polyclonal antibodies were detected using avidin−biotin with biotinylated goat anti-rabbit immunoglobulin as the secondary antibody and horseradish peroxidase-conjugated streptavidin visualized with chromogen diaminobenzidine or tetramethylbenzidine. Monoclonal antibodies were detected using avidin−biotin with biotinylated goat anti-mouse immunoglobulins and secondary antibody and streptavidin conjugated with alkaline phosphatase. Double immunostaining was performed using the Dako EnVision Doublestain System (Dako) following the manufacturer's instructions.

Isolation of Parenchymal and Vascular Amyloid Peptides. Samples of cerebral cortex and cerebellum from a case of sporadic AD (sAD) and a carrier of the *PSEN1* V261I mutation were used in the present study. Approximately 5 g of frontal cortex was dissected free of any large vessel contamination. Amyloid peptides were isolated using a published procedure (*19*) with some modifications. The gray matter was homogenized in a Dounce homogenizer in 10 volumes of TE buffer (0.1 M Tris, pH 7.4, 5 mM EDTA, 0.02% sodium azide) containing protease inhibitors (PI) (Complete, 1 mM pepstatin, 100 mM TLCK−HCl, 200 mM TPCK, and 1 mM leupeptin; all from Roche Molecular Biochemical, Indianapolis, IN) on ice and centrifuged at 200000*g* (Beckman TLA 110 rotor) for 1 h at 4 °C. The supernatant (S_{200}) was stored at −70 °C. The 200000*g* pellet was rehomogenized in 10 volumes of TE buffer with PI. The homogenate was filtered through a series of nylon mesh of 210, 53, and 30 μm to remove small vessel contamination. An equal volume of 30% SDS solution prepared in TE buffer was added to obtain a final concentration of 15% SDS. This solution was stirred overnight at room temperature. The material was centrifuged at 130000*g* for 1 h at 20 °C. The supernatant was centrifuged at 500000*g* for 2 h at 20 °C. The resulting pellet (P_{500}) was dissolved in 99% glass-distilled formic acid for 1 h, and the material was centrifuged for 30 min at 14000*g*. The formic acid soluble material was collected and evaporated under a stream of nitrogen. The pellet resulting from the 130000*g* centrifugation was resuspended in buffer TE with PI and centrifuged at 2000*g* for 15 min. The supernatant from this 2000*g* centrifugation was recentrifuged for 1 h at 130000*g* at 20 °C. The resulting pellet (P_{130A}) was dissolved in formic acid and centrifuged for 30 min at 14000*g*. The formic acid soluble material was collected and evaporated under a stream of nitrogen. The

pellet from the 2000*g* centrifugation was washed in 0.1 M Tris, pH 8.0, four times and digested by collagenase and DNase I (0.3 mg/mL collagenase CLS-3 and 10 μg/mL DNase I; Sigma, St. Louis, MO) in the presence of 2 mM $CaCl_2$ for 16 h at 37 °C. Following digestion, the material was centrifuged at 130000*g* for 1 h at 4 °C. The resulting pellet (P_{130B}) was dissolved in formic acid and centrifugated for 30 min at 14000*g*, and the formic acid soluble fraction was collected and evaporated. Cerebellar tissue, approximately 5 g, was dissected free of any large vessel contamination. The tissue was finely minced and homogenized as described above in 2 volumes of buffer TE with PI and DNase I. The homogenate was centrifuged at 200000*g* for 1 h at 4 °C. The pellet was rehomogenized in 2 volumes of TB buffer with PI. The homogenate was filtered through a series of nylon mesh of 210, 53, and 30 μm to remove small vessel contamination. An equal volume of 30% SDS solution prepared in TE buffer was added to obtain a final concentration of 15% SDS. This solution was stirred overnight at room temperature. The material was centrifuged at 130000*g* for 1 h at 20 °C. The resulting pellet was resuspended in buffer TE with PI and centrifuged at 2000*g* for 15 min. The supernatant from the 2000*g* centrifugation was recentrifuged for 1 h at 130000*g* at 20 °C. The resulting pellet ($P_{130A-Cb}$) was dissolved in formic acid and centrifugated for 30 min at 14000*g*, and the formic acid soluble fraction was evaporated. Leptomeningeal amyloid was isolated using a modification of a published procedure (*22*). Briefly, 3−6 g of vessels was dissected and washed four times at 4 °C with 200 mL of TE buffer and pelleted at 5000*g* for 10 min at 4 °C. Vessels were resuspended in TE buffer and collected by filtration through a 30 μm nylon mesh, washed three times with 100 mL of 1% SDS and 0.1 M Tris, pH 7.4, with PI, and pelleted. Pellets were homogenized in 0.1 M Tris, pH 7.4, with 2 mM $CaCl_2$ and subjected to collagenase/DNase I digestion for 16 h at 37 °C as described above. The digested material was centrifuged at 50000*g*, the resulting pellet (P_{50}) was dissolved in formic acid and centrifugated for 30 min at 14000*g*, and the formic acid soluble fraction was evaporated.

Isolation of CWPs by Laser Microdissection (LMD). Formalin-fixed, paraffin-embedded frontal cortex tissue was used for the isolation of CWPs from two cases of early-onset FAD (*PSEN1* V261I and *PSEN1* V261F). Eight micrometer thick histological sections were placed on membrane-coated slides (Leica Microsystems, Deerfield, IL). Tissue sections were dewaxed twice in xylene for 2 min each, passed through decreasing concentrations of ethanol (100%, 90%, and 70%) and water for 30 s each, stained in eosin for 30 s, and then dehydrated in ethanol. CWPs were dissected using a Leica AS LMD laser microdissection system (Leica Microsystems). Dissected plaques were treated with 99% glass-distilled formic acid in a sealed siliconized tube for 6 h at 96 ± 1 °C using an Eppendorf thermomixer. After incubation, samples were centrifugated for 30 min at 14000*g*, and the formic acid soluble material was collected. The formic acid was evaporated under a stream of nitrogen. For matrix-assisted laser desorption ionization time-of-flight mass spectrometry (MALDI-TOF-MS) analysis, samples were resuspended with 10 μL of an isopropyl alcohol/water/formic acid (4:4:1) mixture and analyzed. For western blot analysis, samples were resuspended in 3× sample buffer and analyzed. A total of about 10000 CWPs were procured for each mass spectrometry analysis, and ∼2500 CWPs were isolated for western blot analysis.

Immunoprecipitation (IP). Fifty microliters of paramagnetic Dynabeads M-450 coated with goat anti-mouse IgG (Dynal Biotech ASA, Oslo, Norway) were allowed to interact for 3 h at room temperature with a mixture of 3 μL of monoclonal antibody 6E10 and 3 μL of monoclonal antibody 4G8 as described (*22*). After incubation, unbound antibody was removed by washing the beads with PBS buffer (10 mM phosphate, pH 7.4, 150 mM NaCl) and 0.1% bovine serum albumin. Supernatant fractions and formic acid extracts (solubilized in 0.5 mL of PBS) were added to the tube containing the coated paramagnetic beads. The samples were incubated overnight at 4 °C. After the incubation, the beads were washed three times with PBS, resuspended in 3× sample buffer with β-mercaptoethanol, and resolved by SDS−PAGE. The beads were also eluted and analyzed by MALDI-TOF-MS.

Identification of the Isolated Components. Proteins and peptides isolated from parenchymal deposits, leptomeningeal vessels, and LMD-CWPs were identified by immunoblot analysis and MALDI-TOF-MS. For western blot analysis, fractions obtained after formic acid extraction were resuspended in 3× sample buffer and resolved by 16% Tris−Tricine SDS−PAGE. Proteins were transferred to poly(vinyl difluoride) (PVDF) membranes using 3-(cyclohexylamino)-1-propanesulfonic acid (CAPS, Sigma), pH 11, containing 10% (v/v) methanol. Membranes were blocked for 1 h with 5% lowfat dried milk in PBS and incubated overnight with the first antibody followed by horseradish peroxidase-labeled goat anti-mouse or anti-rabbit $F(ab')_2$ (1:5000) (Amersham). Immunoblots were visualized with an enhanced chemiluminescence (ECL) detection kit and exposed to Hyperfilm ECL (Amersham). The molecular mass of the Aβ peptides was determined by MALDI-TOF-MS analysis at the New York University Protein Analysis Facility.

Aβ Cross-Linking. Ten percent formalin cross-linked Aβ oligomers were prepared by incubation of 1 mg/mL Aβ1−40 synthetic peptides (Sigma) for 1 and 6 days in 10% formaldehyde at 23 ± 1 °C in a light-protected siliconized microtest vial. As a control, peptides were incubated for the same amount of time in the absence of formaldehyde. The reversal of formaldehyde-induced cross-linking was performed by the addition of 99% formic acid to a final concentration of 5%. After incubation at 96 ± 1 °C for 6 h, samples were analyzed by western blot using the antibody 6E10 (1:1000).

RESULTS

The PSEN1 V261I Mutation Is Associated with Early-Onset FAD. The clinical features and disease progression in the affected individual were consistent with a diagnosis of early-onset FAD. The onset on symptoms was at age 48 years and death occurred at age 55 years. DNA sequencing studies revealed the presence of a G to A nucleotide transition in exon 8 of the *PSEN1* gene (Figure S1, Supporting Information). The mutation is predicted to cause an amino acid change in residue 261 (valine for isoleucine), which is located in the sixth transmembrane domain of the PSEN1 protein. No mutations were observed in exons 16 and 17 of the *AβPP* gene. The *APOE* genotype of the proband was $\epsilon 3\epsilon 3$.

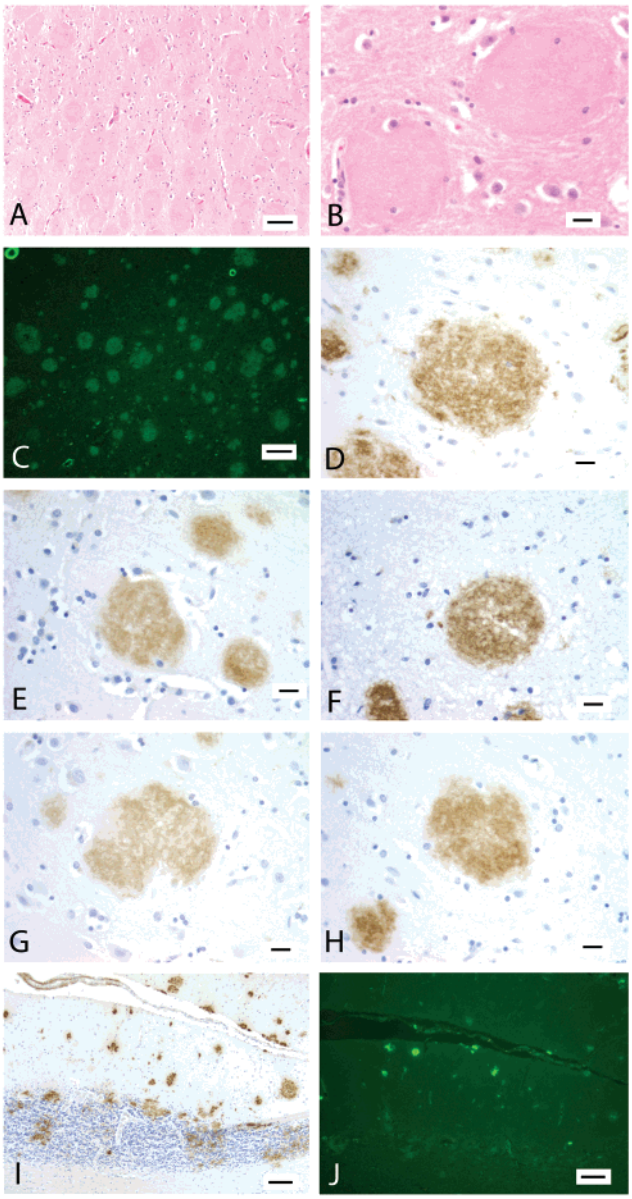

FIGURE 1: Photomicrographs of CWPs from the temporal cortex (A−H) and amyloid deposits from the cerebellum (I, J). (A, B) Numerous well-demarcated CWPs are seen. (C) CWPs are mildly fluorescent. Leptomeningeal vessel walls are intensely fluorescent, indicating the presence of amyloid angiopathy. (D−H) CWPs are immunopositive using a panel of antibodies against different epitopes of the Aβ peptide. (I) Extensive Aβ deposition in the cerebellum. (J) Cerebellar plaques and vessels are intensely fluorescent, but most cerebellar Aβ deposits are mildly fluorescent. (A, B) H&E stain, (C, J) thioflavin S method, and (D−I) immunohistochemistry using antibodies 21F12 (D, I), 6E10 (E), 4G8 (F), HYB310-01 (G), and anti-AβN3pE (H). Bar: 100 μm (A, C, I, J) and 20 μm (B, D−H).

The PSEN1 V261I Mutation Is Associated with Cotton Wool Plaques and Neurofibrillary Tangles. H&E staining and immunohistochemistry revealed the presence of widespread CWPs (Figure 1A,B,D−H) in the neocortex, caudate nucleus, putamen, thalamus, amygdala, hippocampus, parahippocampus, and midbrain. CWPs appeared in the neurophil as round eosinophilic structures lacking dense congophilic amyloid cores (Figure 1A,B). They measured between 80 and 120 μm in diameter. CWPs were weakly fluorescent with Th-S (Figure 1C) and did not show apple-green birefringence

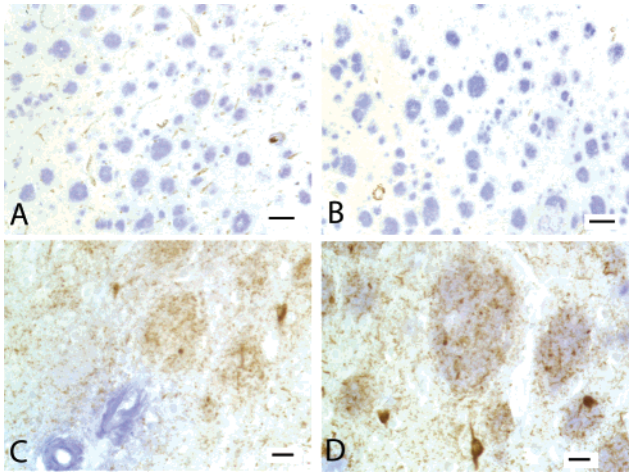

FIGURE 2: Double immunostaining of temporal cortex for AβN−42 (blue) and factor VIII (brown) (A) or αSMA (brown) (B). Double immunostaining of temporal cortex for phosphorylated tau (brown) and AβN−40 (blue) (C) or AβN−42 (blue) (D). Immunohistochemistry was done using antibodies F8/86 (A), 1A4 (B), 21F12 (A, B, D), anti-AβN−40 (C), and AT8 (C, D). Bar: 100 μm (A, B) and 20 μm (C, D).

under polarized light after Congo red staining. CWPs were immunopositive using multiple antibodies against the Aβ peptide (Figure 1D−H). No immunopositivity was seen using antibodies against Aβ peptides ending at position 40 (Figure 2C) and against apolipoprotein E (not shown). In addition to CWPs, occasional neuritic plaques and diffuse deposits were observed. Neuritic plaques were seen predominantly in the neocortex, amygdala, hippocampus, parahippocampus, and substantia innominata. Diffuse amyloid plaques were seen in the neocortex, thalamus, cerebellum, midbrain, pons, and medulla. In the cerebellar molecular layer, both diffuse deposits and cores were present. Diffuse deposits were immunopositive using the panel of antibodies against different epitopes of the Aβ peptide, including antibodies recognizing Aβ peptides ending at position 42 (Figure 1I). The vessel walls of numerous arteries in the leptomeninges, cerebral, and cerebellar parenchyma were thickened and strongly fluorescent in Th-S preparations (Figure 1C,J). Anti-AβN−40 recognized amyloid deposits in parenchymal and leptomeningeal vessels. Factor VIII was used as a marker of vascular endothelial cells (*27*), and αSMA was used as a marker to stain microvessels (*28*). Double immunohistochemistry using antibodies against AβN−42 and factor VIII or αSMA suggested a lack of association between CWPs and blood vessels (Figure 2A,B). Neurofibrillary tangle pathology was widespread in the neocortex, amygdala, hippocampus, and parahippocampus. Double immunohistochemistry using antibodies against phosphorylated tau and AβN−40 or AβN−42 showed that CWPs contained a variable amount of tau-immunoreactive neurites associated with AβN−42 peptide species but not AβN−40 (Figure 2C,D). As previously reported, neurons undergoing neurofibrillary degeneration and large dystrophic neurites similar to those seen in the crown of neuritic plaques were not seen within CWPs (*26*).

Purification and Identification of the Aβ Peptide Species Deposited in PSEN1 V261I. The protocol of purification is outlined under Experimental Procedures (Figure 3). A total of one supernatant (S_{200}) and five pellets (P_{500}, P_{130A}, P_{130B},

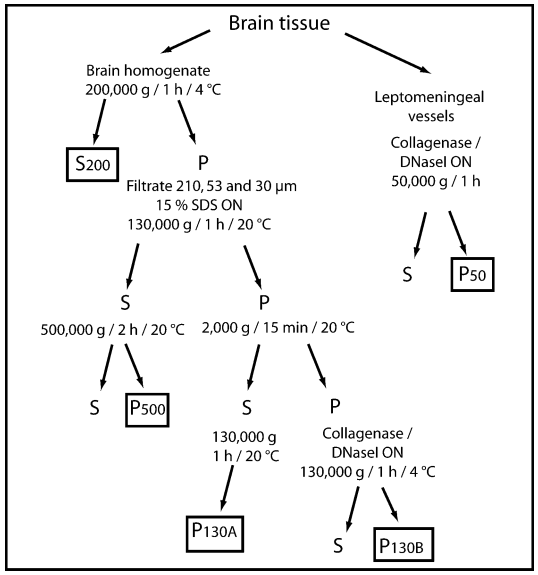

FIGURE 3: Scheme of the amyloid purification protocol. A purification procedure for the isolation of soluble Aβ peptides (S_{200}), parenchymal Aβ deposits (P_{500}, P_{130A}, and P_{130B}) and leptomeningeal Aβ peptides (P_{50}) was performed as outlined and as described in the text.

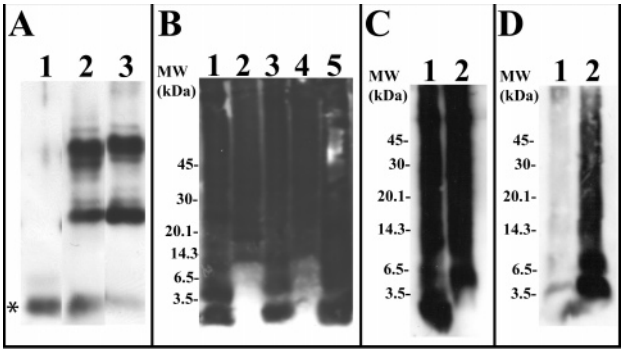

FIGURE 4: Western blots of Aβ peptides isolated from frontal cortex, cerebellum, and leptomeningeal vessels. Equal amounts of protein were loaded on each gel. Peptides were resolved on 16% Tris−Tricine SDS−PAGE. (A) Aβ peptides immunoprecipitated from the S_{200} fraction from the V261I case (lane 2) and a sAD case (lane 3) were reacted against 4G8. The band indicated by an asterisk (*) in lane 1 corresponds to synthetic Aβ1−40 peptide that was run as a control. (B) Aβ peptides isolated from frontal cortex, fractions P_{500} (lane 1), P_{130A} (lane 3), and P_{130B} (lane 5), and Aβ peptides isolated from cerebellum, fractions P_{500-Cb} (lane 2) and $P_{130A-Cb}$ (lane 4), were reacted against 21F12. (C) Immunoprecipitated amyloid fibrils from fraction P_{130A} (lane 1) and fraction P_{50} (lane 2) were reacted against 4G8. (D) Immunoprecipitated amyloid fibrils from fraction P_{130A} (lane 1) and fraction P_{50} (lane 2) were reacted against 3D6. Molecular masses are in kDa.

$P_{130A-Cb}$, and P_{50}) were analyzed to characterize the Aβ peptide species deposited in *PSEN1* V261I−FAD. Aβ1−40 was found to be the predominant Aβ peptide species in the buffer-soluble fraction (S_{200}) from frontal cortex of the *PSEN1* V261I case and in the S_{200} fraction of a sAD case by western blot analysis (Figure 4A, lanes 2 and 3) and by mass spectrometry analysis after IP using a mixture of 4G8 and 6E10 (Figure S2, Supporting Information). The signals corresponding to Aβ3−37, Aβ1−36, Aβ1−37, Aβ1−38, Aβ2−40, and Aβ1−42 were less intense. Western blot analysis of the parenchymal buffer-insoluble/SDS-soluble fraction from the *PSEN1* V261I case after centrifugation at 500000*g* (P_{500}) showed the presence of monomeric and oligomeric forms of the Aβ peptide ending at position 42 and including peptides smaller that 4 kDa (Figure 4B, lane 1). MALDI-TOF-MS of the P_{500} fraction showed the presence of amino-terminally truncated Aβ3−42 and Aβ with a pyroglutamyl residue at position Glu-3 and ending at position 42 (AβN3pE−42) as the predominant Aβ peptide species in this fraction (Figure 5A). In addition, other Aβ peptides were observed in the P_{500} fraction, including Aβ with a pyroglutamyl residue at position Glu-11 and ending at either position 42 (AβN11pE−42) or 43 (AβN11pE−43) and Aβ1−42. The buffer-insoluble/SDS-insoluble fraction obtained after centrifugation at 130000*g* was resuspended and centrifuged at low speed (2000*g*). The supernatant was centrifuged again at 130000*g*, and the insoluble fraction (P_{130A}) was characterized. The P_{130A} fraction contained most of the parenchymal Aβ peptides deposited in the *PSEN1* V261I−FAD. Western blot analysis of the P_{130A} fraction using 21F12 antibodies showed the presence of monomers and oligomers of Aβ ending at position 42 and including peptides smaller that 4 kDa (Figure 4B, lane 3). After IP with 4G8 and 6E10, western blot analysis of the P_{130A} fraction using 4G8 antibodies gave comparable results (Figure 4C, lane 1), suggesting that the peptides smaller than 4 kDa were amino-terminally truncated Aβ peptides. The faint immunoreactivity observed on western blot analysis of the immunoprecipitated P_{130A} fraction using 3D6 antibodies further suggested that the Aβ peptide species present in this fraction were mostly amino-terminally truncated peptides (Figure 4D, lane 1). Monoclonal 3D6 is specific to the amino-terminal region of Aβ that contains the first aspartate residue (*23*). MALDI-TOF-MS of the P_{130A} fraction after IP using a mixture of 4G8 and 6E10 (Figure 5B) or after IP using 21F12 (Figure 5C) showed that the majority of the Aβ peptides present in the P_{130A} fraction were amino-terminally truncated peptides ending at positions 42 and 43. The most intense signals corresponded to AβN11pE−42, AβN11pE−43, AβN3pE−42, and Aβ3−42 peptides, while the signals corresponding to Aβ11−42, Aβ1−42, and Aβ1−43 were less intense. We also observed the presence of Aβ peptide species starting at positions Ala-2, Phe-4, Arg-5, His-6, Asp-7, Ser-8, Gly-9, and Tyr-10. Aβ peptides with ragged amino termini have been seen in senile plaques of sAD patients (*10, 11*). No signal was observed in mass spectrometry after IP of the P_{130A} fraction using anti-AβN−40 (not shown). In contrast, MALDI-TOF-MS of the P_{130A} fraction from the sAD case after IP using a mixture of 4G8 and 6E10 showed that the main peptide present in this fraction was Aβ1−42, followed by AβN3pE−42 and AβN11pE−42 (Figure 5D). Western blot analysis of the 130000*g* pellet (P_{130B}) obtained after collagenase and DNase I digestion of the 2000*g* pellet from the SDS-insoluble fraction showed the presence of aggregated Aβ peptides ending at position 42 and including peptides smaller that 4 kDa (Figure 4B, lane 5). MALDI-TOF-MS of the P_{130B} fraction after IP using a mixture of 4G8 and 6E10 showed the presence of the amino-terminally truncated peptide Aβ3−42 while the signals corresponding to Aβ11−42, Aβ11−43, and Aβ1−42 were less intense (Figure 6A). Similarly, mass spectrometry analysis of the P_{130B} fraction from the control sAD case after IP using a mixture of 4G8 and 6E10 showed the presence of Aβ3−42 while the signals corresponding to Aβ11−42 and Aβ1−42 were less intense (Figure 6B). Western blot analysis using

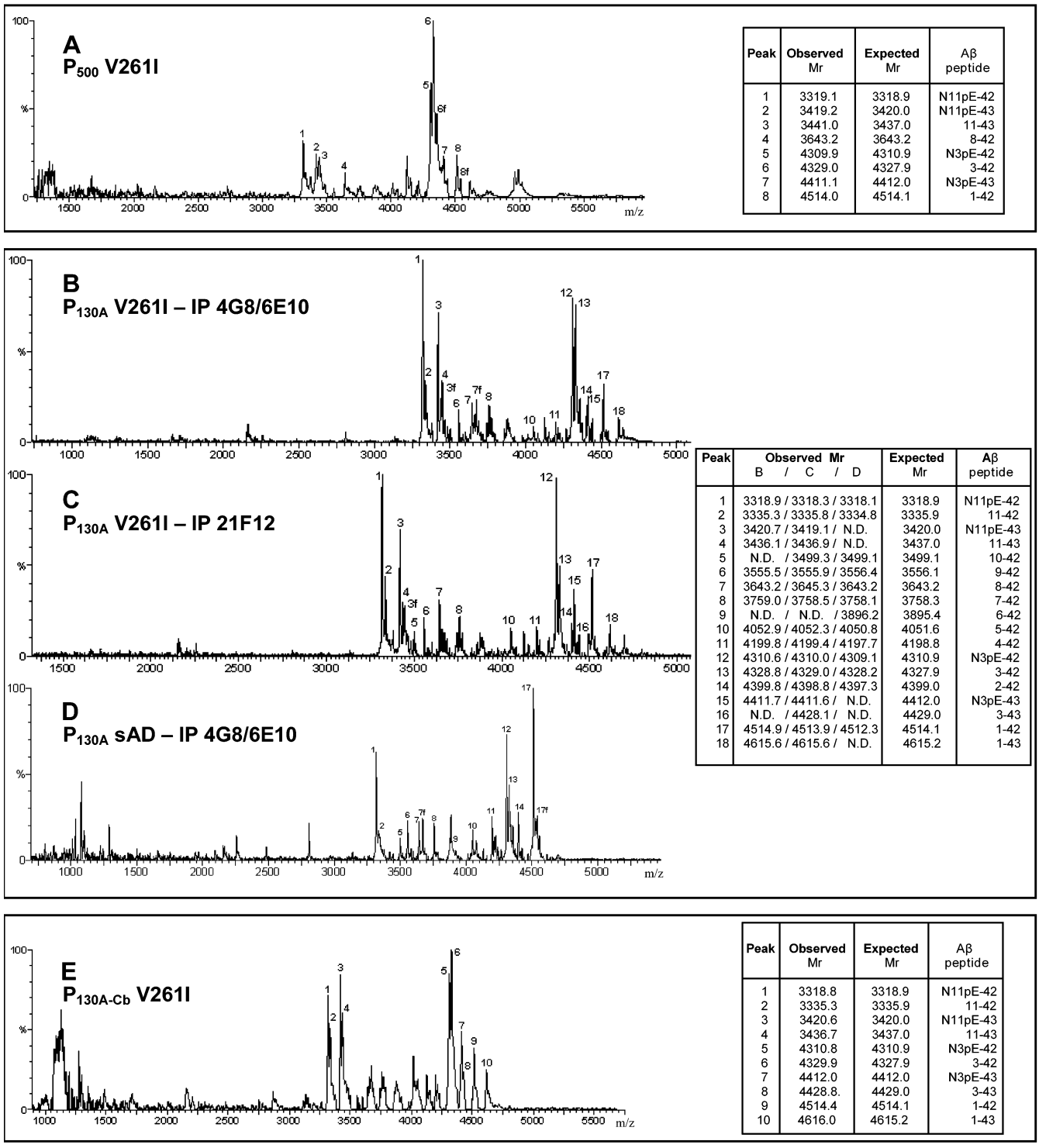

Peak	Observed Mr	Expected Mr	Aβ peptide
1	3319.1	3318.9	N11pE-42
2	3419.2	3420.0	N11pE-43
3	3441.0	3437.0	11-43
4	3643.2	3643.2	8-42
5	4309.9	4310.9	N3pE-42
6	4329.0	4327.9	3-42
7	4411.1	4412.0	N3pE-43
8	4514.0	4514.1	1-42

Peak	Observed Mr B / C / D	Expected Mr	Aβ peptide
1	3318.9 / 3318.3 / 3318.1	3318.9	N11pE-42
2	3335.3 / 3335.8 / 3334.8	3335.9	11-42
3	3420.7 / 3419.1 / N.D.	3420.0	N11pE-43
4	3436.1 / 3436.9 / N.D.	3437.0	11-43
5	N.D. / 3499.3 / 3499.1	3499.1	10-42
6	3555.5 / 3555.9 / 3556.4	3556.1	9-42
7	3643.2 / 3645.3 / 3643.2	3643.2	8-42
8	3759.0 / 3758.5 / 3758.1	3758.3	7-42
9	N.D. / N.D. / 3896.2	3895.4	6-42
10	4052.9 / 4052.3 / 4050.8	4051.6	5-42
11	4199.8 / 4199.4 / 4197.7	4198.8	4-42
12	4310.6 / 4310.0 / 4309.1	4310.9	N3pE-42
13	4328.8 / 4329.0 / 4328.2	4327.9	3-42
14	4399.8 / 4398.8 / 4397.3	4399.0	2-42
15	4411.7 / 4411.6 / N.D.	4412.0	N3pE-43
16	N.D. / 4428.1 / N.D.	4429.0	3-43
17	4514.9 / 4513.9 / 4512.3	4514.1	1-42
18	4615.6 / 4615.6 / N.D.	4615.2	1-43

Peak	Observed Mr	Expected Mr	Aβ peptide
1	3318.8	3318.9	N11pE-42
2	3335.3	3335.9	11-42
3	3420.6	3420.0	N11pE-43
4	3436.7	3437.0	11-43
5	4310.8	4310.9	N3pE-42
6	4329.9	4327.9	3-42
7	4412.0	4412.0	N3pE-43
8	4428.8.	4429.0	3-43
9	4514.4	4514.1	1-42
10	4616.0	4615.2	1-43

FIGURE 5: MALDI-TOF-MS of Aβ peptides isolated from frontal cortex of the V261I case (A−C), from frontal cortex of a sAD control (D), and from cerebellum of the V261I case (E). Fractions P_{500} (A), P_{130A} (B−D), and $P_{130A-Cb}$ (E) were analyzed before (A, E) or after immunoprecipitation with a mixture of 4G8 and 6E10 (B, D) or 21F12 (C). f indicates formylated species (+28 units of mass).

4G8 antibodies of the amyloid extracted from leptomeningeal vessels (P_{50}) showed the presence of 4 kDa monomers and aggregated forms of the Aβ peptide (Figure 4C, lane 2) that were also recognized by the amino-terminal specific antibody 3D6 (Figure 4D, lane 2). Mass spectrometry analysis of the P_{50} fraction showed a major component with a mass of 4329.2 Da corresponding to Aβ1−40 (Figure S3A, Supporting Information). The signals corresponding to Aβ5−40, Aβ1−36, Aβ1−37, Aβ1−38, Aβ2−40, and Aβ1−42 were less intense. MALDI-TOF-MS of the P_{50} fraction after IP with anti-AβN−40 gave identical results (Figure S3B, Supporting Information). Similar Aβ peptide species were observed by mass spectrometry analysis of the P_{50} fraction from the sAD case after IP with 6E10 and 4G8 (Figure S3C, Supporting Information).

Aggregated Amino-Terminally Truncated Aβ Peptide Species Ending at Positions 42 and 43 Are the Predominant Peptides in the Cerebellum in PSEN1 V261I. The same protocol of purification used to isolate cortical Aβ peptides was used to purify cerebellar Aβ deposits. Western blot

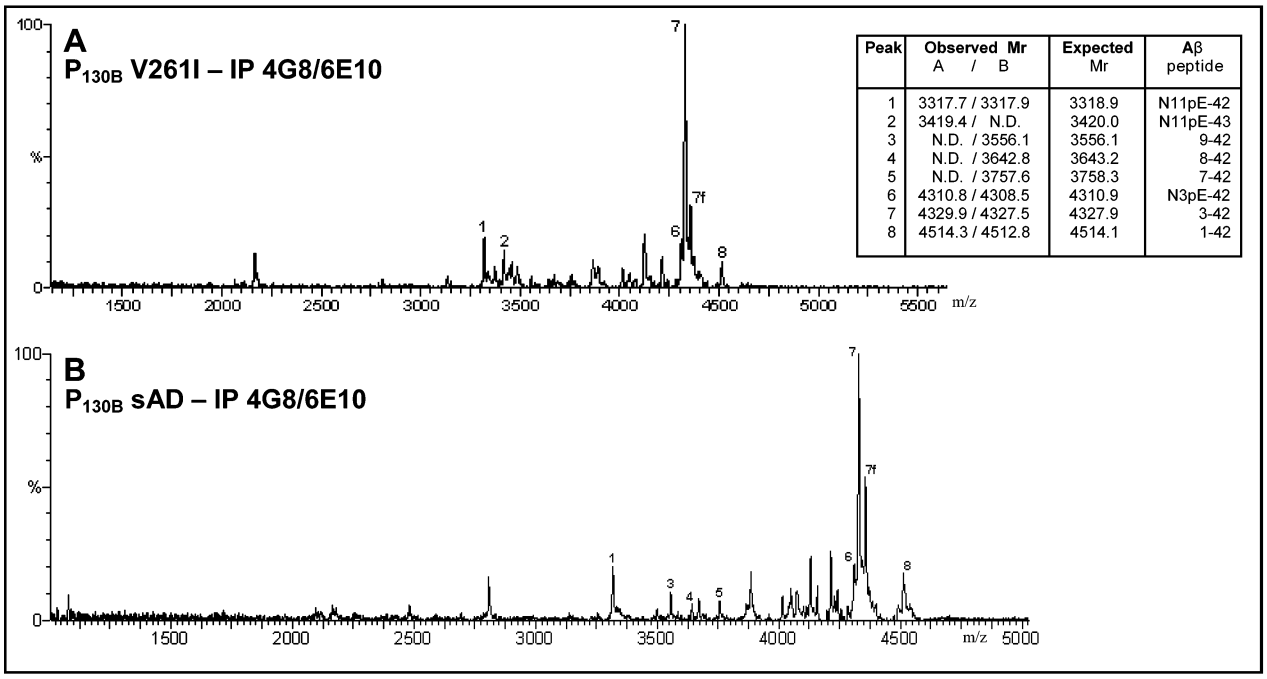

Peak	Observed Mr A / B	Expected Mr	Aβ peptide
1	3317.7 / 3317.9	3318.9	N11pE-42
2	3419.4 / N.D.	3420.0	N11pE-43
3	N.D. / 3556.1	3556.1	9-42
4	N.D. / 3642.8	3643.2	8-42
5	N.D. / 3757.6	3758.3	7-42
6	4310.8 / 4308.5	4310.9	N3pE-42
7	4329.9 / 4327.5	4327.9	3-42
8	4514.3 / 4512.8	4514.1	1-42

FIGURE 6: MALDI-TOF-MS of fraction P_{130B} from the V261I case (A) and from a sAD control (B). Samples were analyzed after immunoprecipitation with a mixture of 4G8 and 6E10. f indicates formylated species (+28 units of mass).

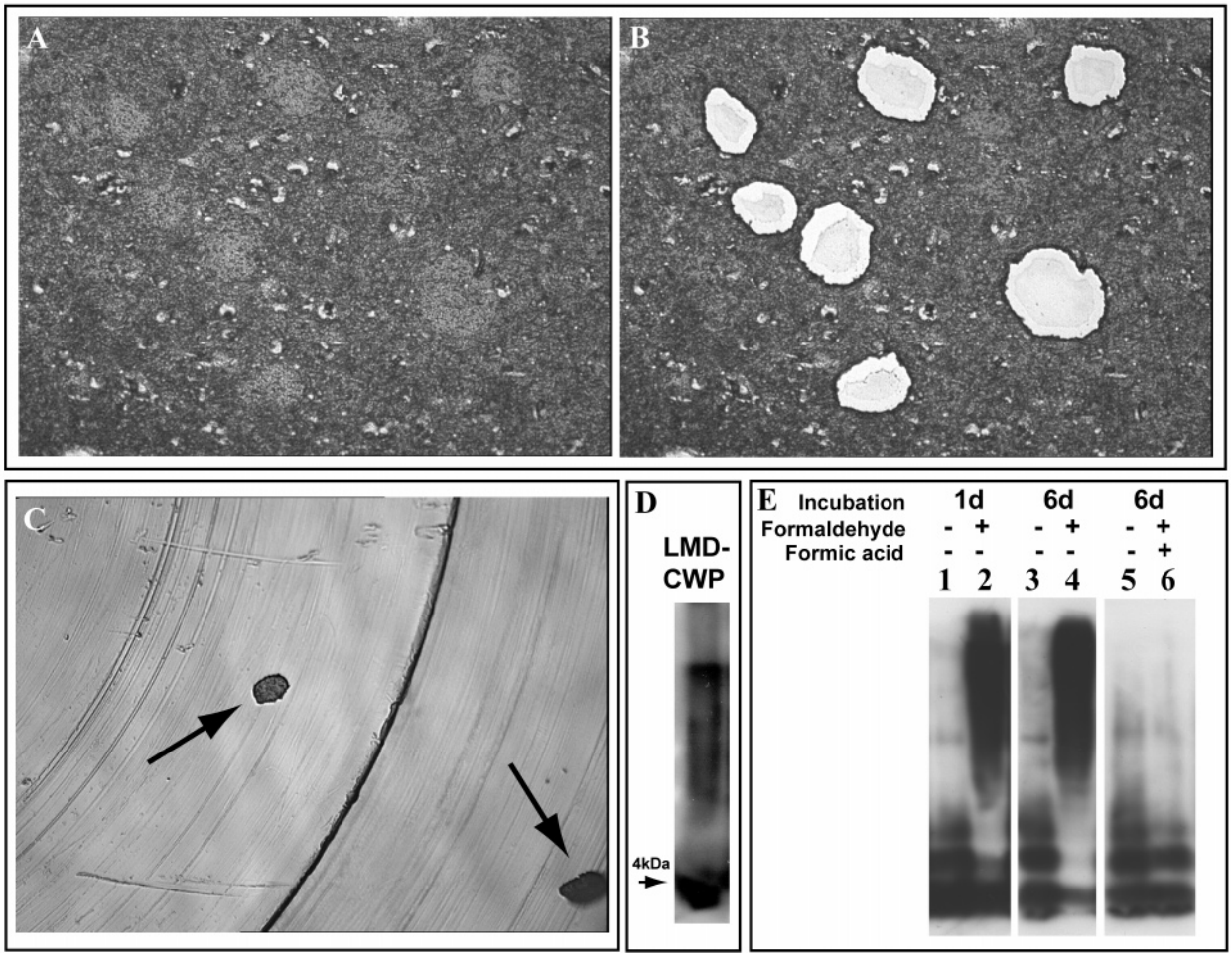

FIGURE 7: Laser microdissection (LMD) of eosin-stained frontal cortex sections. The same section before (A) and after (B) LMD. (C) Captured CWPs on a PCR tube. (D) Western blot of LMD-CWPs reacted against 21F12. (E) Reversal of formaldehyde-induced cross-linking. Synthetic Aβ1−40 peptides (1 mg/mL) were incubated for 1 day (lanes 1, 2) or for 6 days (lanes 3−6) without (lanes 1, 3, 5) or with (lanes 2, 4, 6) the presence of formaldehyde. Formaldehyde-induced cross-linking was reversed by the formic acid−heat treatment (lane 6). Samples were analyzed by western blot using the antibody 6E10.

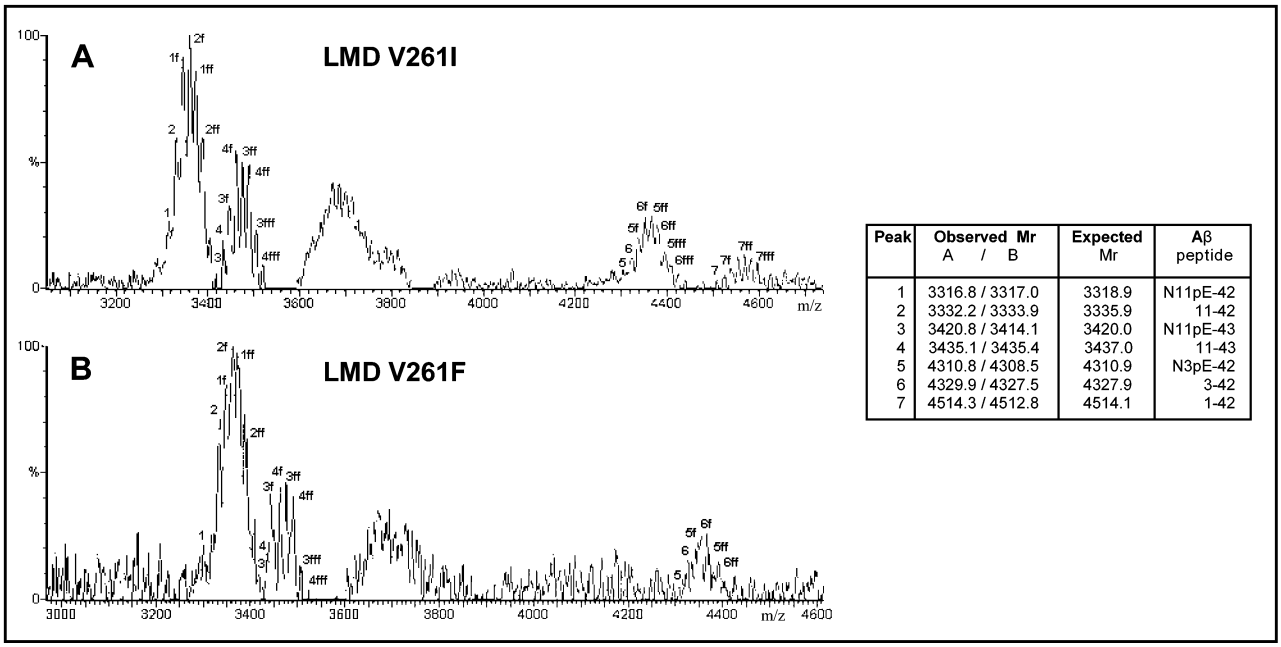

Peak	Observed Mr A / B	Expected Mr	Aβ peptide
1	3316.8 / 3317.0	3318.9	N11pE-42
2	3332.2 / 3333.9	3335.9	11-42
3	3420.8 / 3414.1	3420.0	N11pE-43
4	3435.1 / 3435.4	3437.0	11-43
5	4310.8 / 4308.5	4310.9	N3pE-42
6	4329.9 / 4327.5	4327.9	3-42
7	4514.3 / 4512.8	4514.1	1-42

FIGURE 8: MALDI-TOF-MS of laser microdissected CWPs (~10000) from frontal cortex of the V261I case (A) and the V261F case (B). f indicates formylated species (+28 units of mass).

analysis of the P_{500-Cb} and $P_{130A-Cb}$ fractions obtained from the cerebellum of the *PSEN* V261I case showed the presence of SDS-insoluble oligomeric Aβ peptide aggregates of relative molecular masses over 12 kDa (trimeric form of Aβ) (Figure 4B, lanes 2 and 4). The presence of the oligomeric bands was not affected by the treatment with formic acid. MALDI-TOF-MS of the $P_{130A-Cb}$ fraction showed that the most intense signals corresponded to amino-terminally truncated Aβ peptide species AβN11pE−42, Aβ11−42, AβN11pE−43, Aβ11−43, AβN3pE−42, Aβ3−42, and AβN3pE−43. The signals corresponding to Aβ3−43, Aβ1−42, and Aβ1−43 were less intense (Figure 5E).

Identification of the Aβ Peptide Species Present in CWPs Isolated by Laser Microdissection (LMD-CWPs). Eosin-stained CWPs were microdissected from formaldehyde-fixed sections (Figure 7A−C). Approximately, 2500 plaques from the *PSEN1* V261I−FAD case were cut and treated over a 6 h period using formic acid to reverse the cross-linking of the amyloid peptides. Western blot analysis of the formic acid soluble material showed the presence of AβN−42 peptide species smaller than 4 kDa (Figure 7D). Since formaldehyde cross-links proteins to each other primarily between the ϵ-amino group of lysine residues and an adjacent peptide bond (Aβ has two lysine residues at positions 16 and 28), we reversed the cross-links by high-temperature heating and formic acid treatment (*29*). To control for the formic acid/heat treatment to reverse the cross-links introduced by the fixative, Aβ oligomers were prepared by incubation of Aβ1−40 synthetic peptides for 1 day and for 6 days in 10% formaldehyde. After 24 h, most of the Aβ peptides incubated in the presence of formaldehyde migrated as high molecular mass oligomers (Figure 7E, lane 2). After 6 days of incubation, the majority of the Aβ peptides incubated in the presence of formaldehyde were cross-linked (Figure 7E, lane 4). After 6 days of incubation, the addition of formic acid and further incubation at 96 ± 1 °C for 6 h completely reversed the cross-linking process (Figure 7E, lane 6). No signs of peptide degradation due to the formic acid treatment were observed. Approximately 10000 CWPs were isolated by LMD from frontal cortex of the *PSEN1* V261I individual. In addition, ~10000 CWPs were isolated by LMD from frontal cortex of an individual with the *PSEN1* V261F mutation, which is also characterized by the presence of CWPs (*30*). Isolated CWPs were treated with formic acid, and the soluble material was analyzed by MALDI-TOF-MS (Figure 8). In both cases, the main peptides detected were the amino-terminally truncated Aβ peptides AβN11pE−42 and Aβ11−42. Other Aβ peptide species included AβN11pE−43, Aβ11−43, AβN3pE−42, and Aβ3−42. The signal corresponding to Aβ1−42 was very weak. A high degree of formylation was observed. We are uncertain about the identity of the peptides between 3600 and 3960 units of mass. We speculate that these peptides may represent formylated species of Aβ3−34 and AβN3pE−34, which have 3600.9 and 3584.9 units of mass, respectively.

CONCLUSIONS

In the present study, we examined the amyloid peptides present in an individual carrier of a novel missense (V261I) mutation in the *PSEN1* gene that is associated with early-onset FAD. In the cerebral cortex, numerous CWPs and neurofibrillary tangles were found. Immunohistological studies, western blot analysis, and MALDI-TOF-MS analysis of the amyloid peptides isolated from the cerebral cortex and from LMD-CWPs suggest that CWPs contain an array of amino-terminally truncated Aβ peptide species ending at residues 42 and 43. In the cerebellum, diffuse amyloid plaques were found. MALDI-TOF-MS analysis of the amyloid peptides isolated from the cerebellum showed that these deposits contain an array of amino-terminally truncated Aβ peptide species similar to the one observed in the cerebral cortex and in LMD-CWPs. In addition, we identified Aβ1−40 as the main Aβ peptide species in the soluble pool of the cerebral cortex and in amyloid deposits in leptomeningeal vessels.

Senile plaques, a neuropathological hallmark of AD, have been extensively studied. However, the biochemical composition of other types of plaques is still unknown (*31*). The characterization of plaques that are morphologically different from senile plaques is important for the understanding of the role that amyloid peptides play in the disease process. CWPs are round eosinophilic plaques that lack a central amyloid core and are mildly fluorescent on Th-S preparations. Immunohistological studies using the end-specific anti-AβN−40 antibody and antibodies against vascular markers suggest that vessels do not participate in the structure of this type of plaque. To characterize the Aβ peptide species present in CWPs, we used biochemical methods for the isolation of parenchymal amyloid peptides and LMD for the isolation of individual CWPs. Laser microdissection has been recently used to quantify the Aβ peptides in senile plaques in sAD (*32*) and for the proteomic characterization of amyloid plaques in sAD (*33*). LMD allowed us to obtain a pure preparation of CWPs for western blot and MALDI-TOF-MS analysis. Our results indicate that CWPs are composed predominantly by amino-terminally truncated Aβ peptide species with or without a pyroglutamyl residue at positions Glu-3 and Glu-11 and ending at positions 42 and 43. Full-length Aβ1−42 and Aβ1−43 peptide species were underrepresented. The MALDI-TOF-MS studies allowed the identification of the amyloid peptide species that were present in the amyloid deposits and to obtain semiquantitative information of the peptides present in the samples. To obtain quantitative information by MALDI-TOF-MS is very difficult due to the degree of complexity of the samples and the presence of substances that may cause suppression of signals from some ionic species. The identification and characterization of Aβ peptide species with structural alterations in the peptide backbone (*11*) were not in the scope of our studies.

MALDI-TOF-MS of CWPs did not show the presence of Aβ1−40, which was also confirmed by the immunohistological studies. The lack of Aβ1−40 in CWPs strongly suggests that CWPs are not associated with vascular structures. The absence of Aβ17−42 (p3) suggests that CWPs are not related to the deposition of p3, a major component of diffuse plaques in the cerebral cortex of sAD (*19*, *20*) and in the cerebellar cortex of DS patients (*34*). Aβ peptides starting with pyroglutamyl at residues Glu-3 and Glu-11, particularly AβN3pE−42, have been suggested to be early aggregating species in AD (*12*, *14*) and to be more abundant in patients with *PSEN1* mutations than in patients with sAD (*15*). The exact location (intracellular vs extracellular) where glutamate is converted into pyroglutamate is not known, but the loss of three charges, including an amino-terminal charge for AβN3pE−42 and six charges for AβN11pE−42, has a significant effect on the conformational behavior and depositability of these peptides, which aggregate more rapidly than full-length Aβ1−42 (*35*). These amino-terminally truncated variants of Aβ were not generated by protein degradation during the purification of the peptides since we used protease inhibitors during all of the purification steps. They were also not generated by formic acid treatment of the amyloid peptides since amino-terminal truncated variants of Aβ have not been seen after treatment of synthetic Aβ peptides with formic acid (*22*, *36*, *37*). The analysis of the cerebellar amyloid deposits associated with the *PSEN1* V261I mutation showed that they contain an array of Aβ peptide species similar to that observed in the cerebral cortex. We observed the presence of Aβ peptides starting with pyroglutamyl at residues Glu-3 and Glu-11 and ending at positions 42 and 43 as the main component of the cerebellar deposits, suggesting that the cerebrum and the cerebellum produce a similar array of Aβ peptide species. Interestingly, western blot analysis of the cerebellar amyloid peptides revealed a pattern of immunoreactivity different from the pattern of immunoreactivity of the cerebral cortical amyloid, showing the presence of mostly detergent-insoluble oligomers of Aβ peptides. This observation suggests that the extracellular environment may play an important role in the aggregation of the Aβ peptides and that the differences at the morphological level (e.g., CWPs in the cerebral cortex vs diffuse deposits in the cerebellum) might reflect the presence of cell- or region-specific factors. A similar array of cerebellar Aβ peptide species were reported by Iwatsubo et al. (*17*) in diffuse plaques of the cerebellum of sAD and DS patients and in nondemented individuals analyzed by immunohistochemistry using a panel of well-characterized antibodies to Aβ, although Aβ peptides starting at residue Glu-11 were only occasionally seen (*17*). Taken together, these results suggest that the carrier of the *PSEN1* V261I mutation may overproduce Aβ peptides starting at positions Glu-3 and Glu-11, in particular AβN11pE−42(43), in agreement with the report by Russo et al. (*15*) indicating that AβN11pE−42(43) was significantly increased in subjects carrying mutations in the *PSEN1* gene. Aβ peptides starting at position Glu-11 are known to contribute to the total Aβ levels in elderly normal human brains, preclinical AD, and AD (*10*, *13*, *38*). Peptides starting at position Glu-11 have also been found in the brain of transgenic animals overexpressing the *AβPP* V717I mutation (*39*) and are a minor component of the brain deposits in a transgenic animal model carrying the double Swedish mutation under the control of the *Thy-1* promoter (*40*). Peptides starting at position Glu-11 were not found in an animal model carrying the double Swedish mutation under the control of the hamster *prion protein* promoter (*37*). Aβ peptides beginning with Glu-11 are derived from the cleavage of AβPP by BACE1 (*2*). BACE1 cleavage of AβPP between Tyr-10 and Glu-11 within the Aβ domain (β'-cleavage) results in the secretion of an amino-terminal ectodomain, sAβPPβ', and the retention of an 89 amino acid CTF, C89. C89 can also be produced by proteolysis by BACE1 at Glu-11 of C99, which results from BACE1 cleavage of AβPP between methionine and aspartate at position 1 of the amino terminus of Aβ (β-cleavage) (*41*). The membrane-bound CTFs of AβPP are then subjected to further proteolysis within the transmembrane domain by γ-secretase, generating the Aβ peptide species ending at either amino acid 40 or amino acid 42. Whereas all of the components of γ-secretase have not been identified, the presenilin proteins are necessary for secretion of Aβ peptides and have been postulated to contain the active site of γ-secretase (*1*). Increased BACE1 expression has been implicated in the pathogenesis of AD (*42*), and in vitro studies have shown that the overexpression of BACE1 results in enhanced production of Aβ peptides beginning at Glu-11 (*41*). In the brain of BACE1 x AβPP V717I double-transgenic mice, amyloidogenic processing at both Asp-1 and Glu-11 was found to be increased, resulting in more and

different Aβ peptide species and CTFs (*43*). BACE1 significantly increased the number of diffuse and senile amyloid plaques in old double-transgenic mice but lowered vascular amyloid deposition, suggesting an inverse relation of vascular amyloid to the levels of the less soluble amino-terminally truncated Aβ (*43*). However, a diminished deposition of Aβ peptides despite enhanced β-cleavage of AβPP has been recently reported in a transgenic animal model overexpressing BACE1 (*44*). The authors postulated that BACE1 overexpression altered the subcellular localization of BACE1 cleavage by increasing β-cleavage early in the secretory pathway, thereby depleting AβPP destined for axonal transport, highlighting the importance of the subcellular site of Aβ generation in the pathogenesis of AD (*44*).

We found a soluble pool of Aβ peptide species (sAβ), which was operationally defined as Aβ peptides extracted from brain cortex under mild conditions (i.e., homogenated in 100 mM Tris, pH 7.4, with PI) after centrifugation at 200000*g*. MALDI-TOF-MS analysis of the buffer-soluble Aβ fraction revealed that Aβ1−40 was the main Aβ peptide species in this fraction, which is in agreement with previous reports indicating that Aβ1−40 is the main sAβ peptide species in the presence of a high degree of cerebral amyloid angiopathy (CAA) (*45*). Our results suggest that sAβ peptide species may contribute significantly to the development of CAA associated with the *PSEN1* V261I mutation since MALDI-TOF-MS analysis of the Aβ peptide species present in leptomeningeal vessels showed that Aβ1−40 is the main Aβ peptide species in this fraction. Furthermore, other minor Aβ peptide species such as Aβ1−36, Aβ1−37, Aβ1−38, and Aβ2−40 were also present in both the soluble fraction and the vascular deposits. Fewer species of amino-terminally truncated AβN−40 peptides than amino-terminally truncated AβN−42 peptides were observed in association with the *PSEN1* V261I mutation. This finding suggests that amino-terminally truncated AβN−40 and AβN−42 peptides may be generated by different proteolytic mechanisms or that amino-terminally truncated AβN−40 peptides are rapidly degraded. The biochemical and pathological data together clearly demonstrate that there is a differential contribution of amyloid peptides of different lengths to the development of the parenchymal and vascular amyloid pathology associated with the *PSEN1* V261I mutation.

As a molecular mechanism, mutations in the *PSEN1* gene have been proposed to alter the normal processing of AβPP leading to abnormally high levels of production of Aβ1−42(43) (*46*). However, it is extremely puzzling that the over 140 mutations in the *PSEN1* gene (http://www.molgen.ua.ac.be/) have the unique property of enhancing the cleavage of AβPP at the γ-secretase site of AβPP. Moreover, not all of the mutations lead to increased levels of Aβ1−42(43) (*47*), and some families with *PSEN1* mutations may present with clinical and neuropathological features remarkably different from "typical" AD. One example of an "atypical" neuropathologic phenotype associated with a *PSEN1* mutation is the case of FAD associated with CWPs. We propose that mutations in the *PSEN1* gene may alter the pathway(s) involved in the generation of Aβ peptide species, as to favor the production of particular arrays of full-length and amino-terminally truncated Aβ peptide species ending at residues 42(43). The biochemical composition of the Aβ peptides produced in association with each mutation may constitute the structural basis for the morphological diversity of amyloid deposits seen in *PSEN1*−FAD and, perhaps, in some *AβPP*−FAD. Recently, the Aβ peptide species present in three individuals carrying the *AβPP* V717F mutation have been characterized (*48*). Neuropathologically, individuals carrying the *AβPP* V717F mutation are characterized by the presence of flocculent amyloid plaques and an almost complete absence of compact amyloid cores. The biochemical analysis of the flocculent amyloid plaques showed that these plaques are composed of longer Aβ peptide species with carboxyl termini between residues 43 and 54 (*48*). These data further support a primary role for amyloid peptides of different lengths in determining the morphological appearance of amyloid plaques. Thus, the generation of highly insoluble amino-terminally truncated Aβ peptides seen in association with the *PSEN1* V261I and *PSEN1* V261F mutations may be of major importance in the pathological process of early onset FAD and must be taken into consideration when developing new diagnostic and therapeutic strategies for AD.

ACKNOWLEDGMENT

The authors gratefully acknowledge the help of C. A. Rentz, the technical help of R. Richardson and B. Dupree, and the photographic assistance of U. Küderli. The authors are grateful to Y. Lu and T. Neubert at the New York University Protein Analysis Facility, Skirball Institute, New York University School of Medicine, New York.

SUPPORTING INFORMATION AVAILABLE

Direct sequencing of a PCR product showing the nucleotide substitution in the *PSEN1* gene and MALDI-TOF-MS of the soluble fractions and leptomeningeal vessels. This material is available free of charge via the Internet at http://pubs.acs.org.

REFERENCES

1. Selkoe, D. J. (2001) Alzheimer's disease: genes, proteins, and therapy, *Physiol. Rev. 81*, 741−766.
2. Vassar, R., Bennett, B. D., Babu-Khan, S., Kahn, S., Mendiaz, E. A., Denis, P., Teplow, D. B., Ross, S., Amarante, P., Loeloff, R., Luo, Y., Fisher, S., Fuller, J., Edenson, S., Lile, J., Jarosinski, M. A., Biere, A. L., Curran, E., Burgess, T., Louis, J. C., Collins, F., Treanor, J., Rogers, G., and Citron, M. (1999) Beta-secretase cleavage of Alzheimer's amyloid precursor protein by the transmembrane aspartic protease BACE, *Science 286*, 735−741.
3. Gu, Y., Sanjo, N., Chen, F., Hasegawa, H., Petit, A., Ruan, X., Li, W., Shier, C., Kawarai, T., Schmitt-Ulms, G., Westaway, D., St. George-Hyslop, P., and Fraser, P. E. (2004) The presenilin proteins are components of multiple membrane-bound complexes that have different biological activities, *J. Biol. Chem. 279*, 31329−31336.
4. Pike, C. J., Burdick, D., Walencewicz, A. J., Glabe, C. G., and Cotman, C. W. (1993) Neurodegeneration induced by beta-amyloid peptides in vitro: the role of peptide assembly state, *J. Neurosci. 13*, 1676−1687.
5. Younkin, S. G. (1995) Evidence that Aβ 42 is the real culprit in Alzheimer's disease, *Ann. Neurol. 37*, 287−288.
6. Klein, W. L. (2002) Abeta toxicity in Alzheimer's disease: globular oligomers (ADDLs) as new vaccine and drug targets, *Neurochem. Int. 41*, 345−352.
7. Dahlgren, K. N., Manelli, A. M., Stine, W. B., Baker, L. K., Krafft, G. A., and LaDu, M. J. (2002) Oligomeric and fibrillar species of amyloid-beta peptides differentially affect neuronal viability, *J. Biol. Chem. 277*, 32046−32053.
8. Masters, C. L., Simms, G., Weinman, N. A., Multhaup, G., McDonald, B. L., and Beyreuther, K. (1985) Amyloid plaque core

protein in Alzheimer disease and Down syndrome, *Proc. Natl. Acad. Sci. U.S.A. 82*, 4245−4249.
9. Mori, H., Takio, K., Ogawara, M., and Selkoe, D. J. (1992) Mass spectrometry of purified amyloid beta protein in Alzheimer's disease, *J. Biol. Chem. 267*, 17082−17086.
10. Miller, D. L., Papayannopoulos, I. A., Styles, J., Bobin, S. A., Lin, Y. Y., Biemann, K., and Iqbal, K. (1993) Peptide compositions of the cerebrovascular and senile plaque core amyloid deposits of Alzheimer's disease, *Arch. Biochem. Biophys. 301*, 41−52.
11. Roher, A. E., Lowenson, J. D., Clarke, S., Wolkow, C., Wang, R., Cotter, R. J., Reardon, I. M., Zurcher-Neely, H. A., Heinrikson, R. L., Ball, M. J., and Greenberg, B. D. (1993) Structural alterations in the peptide backbone of beta-amyloid core protein may account for its deposition and stability in Alzheimer's disease, *J. Biol. Chem. 268*, 3072−3083.
12. Kuo, Y. M., Emmerling, M. R., Woods, A. S., Cotter, R. J., and Roher, A. E. (1997) Isolation, chemical characterization, and quantitation of A beta 3-pyroglutamyl peptide from neuritic plaques and vascular amyloid deposits, *Biochem. Biophys. Res. Commun. 237*, 188−191.
13. Naslund, J., Schierhorn, A., Hellman, U., Lannfelt, L., Roses, A. D., Tjernberg, L. O., Silberring, J., Gandy, S. E., Winblad, B., Greengard, P., Nordstedt, C., and Terenius, L. (1994) Relative abundance of Alzheimer A beta amyloid peptide variants in Alzheimer disease and normal aging, *Proc. Natl. Acad. Sci. U.S.A. 91*, 8378−8382.
14. Tekirian, T. L. (2001) Abeta N-Terminal Isoforms: Critical contributors in the course of AD pathophysiology, *J. Alzheimer's Dis. 3*, 241−248.
15. Russo, C., Schettini, G., Saido, T. C., Hulette, C., Lippa, C., Lannfelt, L., Ghetti, B., Gambetti, P., Tabaton, M., and Teller, J. K. (2000) Presenilin-1 mutations in Alzheimer's disease, *Nature 405*, 531−532.
16. Saido, T. C., Iwatsubo, T., Mann, D. M., Shimada, H., Ihara, Y., and Kawashima, S. (1995) Dominant and differential deposition of distinct beta-amyloid peptide species, A beta N3(pE), in senile plaques, *Neuron 14*, 457−466.
17. Iwatsubo, T., Saido, T. C., Mann, D. M., Lee, V. M., and Trojanowski, J. Q. (1996) Full-length amyloid-beta (1−42(43)) and amino-terminally modified and truncated amyloid-beta 42-(43) deposit in diffuse plaques, *Am. J. Pathol. 149*, 1823−1830.
18. Gouras, G. K., Xu, H., Jovanovic, J. N., Buxbaum, J. D., Wang, R., Greengard, P., Relkin, N. R., and Gandy, S. (1998) Generation and regulation of beta-amyloid peptide variants by neurons, *J. Neurochem. 71*, 1920−1925.
19. Gowing, E., Roher, A. E., Woods, A. S., Cotter, R. J., Chaney, M., Little, S. P., and Ball, M. J. (1994) Chemical characterization of A beta 17−42 peptide, a component of diffuse amyloid deposits of Alzheimer disease, *J. Biol. Chem. 269*, 10987−10990.
20. Higgins, L. S., Murphy, G. M., Jr., Forno, L. S., Catalano, R., and Cordell, B. (1996) P3 beta-amyloid peptide has a unique and potentially pathogenic immunohistochemical profile in Alzheimer's disease brain, *Am. J. Pathol. 149*, 585−596.
21. Prelli, F., Castaño, E. M., Glenner, G. G., and Frangione, B. (1988) Differences between vascular and plaque core amyloid in Alzheimer's disease, *J. Neurochem. 51*, 648−651.
22. Vidal, R., Calero, M., Piccardo, P., Farlow, M. R., Unverzagt, F. W., Mendez, E., Jimenez-Huete, A., Beavis, R., Gallo, G., Gomez-Tortosa, E., Ghiso, J., Hyman, B. T., Frangione, B., and Ghetti, B. (2000) Senile dementia associated with amyloid beta protein angiopathy and tau perivascular pathology but not neuritic plaques in patients homozygous for the APOE-epsilon4 allele, *Acta Neuropathol. (Berlin) 100*, 1−12.
23. Johnson-Wood, K., Lee, M., Motter, R., Hu, K., Gordon, G., Barbour, R., Khan, K., Gordon, M., Tan, H., Games, D., Lieberburg, I., Schenk, D., Seubert, P., and McConlogue, L. (1997) Amyloid precursor protein processing and A beta 42 deposition in a transgenic mouse model of Alzheimer disease, *Proc. Natl. Acad. Sci. U.S.A. 94*, 1550−1555.
24. Frenkel, D., Balass, M., and Solomon, B. (1998) N-terminal EFRH sequence of Alzheimer's beta-amyloid peptide represents the epitope of its anti-aggregating antibodies, *J. Neuroimmunol. 88*, 85−90.
25. Jimenez-Huete, A., Alfonso, P., Soto, C., Albar, J. P., Rabano, A., Ghiso, J., Frangione, B., and Mendez, E. (1998) Antibodies directed to the carboxyl terminus of amyloid β-peptide recognize sequence epitopes and distinct immunoreactive deposits in Alzheimer's disease brain, *Alzheimer Rep. 1*, 41−48.
26. Takao, M., Ghetti, B., Hayakawa, I., Ikeda, E., Fukuuchi, Y., Miravalle, L., Piccardo, P., Murrell, J. R., Glazier, B. S., and Koto, A. (2002) A novel mutation (G217D) in the Presenilin 1 gene (PSEN1) in a Japanese family: presenile dementia and parkinsonism are associated with cotton wool plaques in the cortex and striatum, *Acta Neuropathol. (Berlin) 104*, 155−170.
27. Sehested, M., and Hou-Jensen, K. (1981) Factor VII related antigen as an endothelial cell marker in benign and malignant diseases, *Virchows Arch. A: Pathol. Anat. Histol. 391*, 217−225.
28. Skalli, O., Ropraz, P., Trzeciak, A., Benzonana, G., Gillessen, D., and Gabbiani, G. (1986) A monoclonal antibody against alpha-smooth muscle actin: a new probe for smooth muscle differentiation, *J. Cell Biol. 103*, 2787−2796.
29. Shi, S. R., Cote, R. J., and Taylor, C. R. (1997) Antigen retrieval immunohistochemistry: past, present, and future, *J. Histochem. Cytochem. 45*, 327−343.
30. Farlow, M., Murrell, J. R., Unverzagt, F. W., Phillips, M., Takao, M., and Ghetti, B. (2001) Familial Alzheimer's disease with spastic paraparesis associated with a mutation at codon 261 of the presenilin 1 gene, in *Alzheimer's disease: advances in etiology, pathogenesis and therapeutics* (Iqbal, K., Sisodia, S. S., and Winblad, B., Eds), pp 53−60, John Wiley & Sons, Chichester.
31. Dickson, D. W. (1997) The pathogenesis of senile plaques, *J. Neuropathol. Exp. Neurol. 56*, 321−339.
32. Rufenacht, P., Guntert, A., Bohrmann, B., Ducret, A., and Dobeli, H. (2005) Quantification of the A beta peptide in Alzheimer's plaques by laser dissection microscopy combined with mass spectrometry, *J. Mass Spectrom. 40*, 193−201.
33. Liao, L., Cheng, D., Wang, J., Duong, D. M., Losik, T. G., Gearing, M., Rees, H. D., Lah, J. J., Levey, A. I., and Peng, J. (2004) Proteomic characterization of postmortem amyloid plaques isolated by laser capture microdissection, *J. Biol. Chem. 279*, 37061−37068.
34. Lalowski, M., Golabek, A., Lemere, C. A., Selkoe, D. J., Wisniewski, H. M., Beavis, R. C., Frangione, B., and Wisniewski, T. (1996) The "nonamyloidogenic" p3 fragment (amyloid beta17−42) is a major constituent of Down's syndrome cerebellar preamyloid, *J. Biol. Chem. 271*, 33623−33631.
35. He, W., and Barrow, C. J. (1999) The A beta 3-pyroglutamyl and 11-pyroglutamyl peptides found in senile plaque have greater beta-sheet forming and aggregation propensities in vitro than full-length A beta, *Biochemistry 38*, 10871−10877.
36. Delacourte, A., Sergeant, N., Champain, D., Wattez, A., Maurage, C. A., Lebert, F., Pasquier, F., and David, J. P. (2002) Nonoverlapping but synergetic tau and APP pathologies in sporadic Alzheimer's disease, *Neurology 59*, 398−407.
37. Kalback, W., Watson, M. D., Kokjohn, T. A., Kuo, Y. M., Weiss, N., Luehrs, D. C., Lopez, J., Brune, D., Sisodia, S. S., Staufenbiel, M., Emmerling, M., and Roher, A. E. (2002) APP transgenic mice Tg2576 accumulate Aβ peptides that are distinct from the chemically modified and insoluble peptides deposited in Alzheimer's disease senile plaques, *Biochemistry 41*, 922−928.
38. Sergeant, N., Bombois, S., Ghestem, A., Drobecq, H., Kostanjevecki, V., Missiaen, C., Wattez, A., David, J. P., Vanmechelen, E., Sergheraert, C., and Delacourte, A. (2003) Truncated beta-amyloid peptide species in pre-clinical Alzheimer's disease as new targets for the vaccination approach, *J. Neurochem. 85*, 1581−1591.
39. Pype, S., Moechars, D., Dillen, L., and Mercken, M. (2003) Characterization of amyloid beta peptides from brain extracts of transgenic mice overexpressing the London mutant of human amyloid precursor protein, *J. Neurochem. 84*, 602−609.
40. Kuo, Y. M., Kokjohn, T. A., Beach, T. G., Sue, L. I., Brune, D., Lopez, J. C., Kalback, W. M., Abramowski, D., Sturchler-Pierrat, C., Staufenbiel, M., and Roher, A. E. (2001) Comparative analysis of amyloid-beta chemical structure and amyloid plaque morphology of transgenic mouse and Alzheimer's disease brains, *J. Biol. Chem. 276*, 12991−12998.
41. Liu, K., Doms, R. W., and Lee, V. M. (2002) Glu11 site cleavage and N-terminally truncated A beta production upon BACE overexpression, *Biochemistry 41*, 3128−3136.
42. Holsinger, R. M., McLean, C. A., Beyreuther, K., Masters, C. L., and Evin, G. (2002) Increased β-Secretase activity in cerebrospinal fluid of Alzheimer's disease subjects, *Ann. Neurol. 51*, 783−786.
43. Willem, M., Dewachter, I., Smyth, N., Van Dooren, T., Borghgraef, P., Haass, C., and Van Leuven, F. (2004) beta-site amyloid precursor protein cleaving enzyme 1 increases amyloid deposition in brain parenchyma but reduces cerebrovascular amyloid angi-

opathy in aging BACE x APP[V717I] double-transgenic mice, *Am. J. Pathol. 165*, 1621−1631.
44. Lee, E. B., Zhang, B., Liu, K., Greenbaum, E. A., Doms, R. W., Trojanowski, J. Q., and Lee, V. M. (2005) BACE overexpression alters the subcellular processing of APP and inhibits Aβ deposition in vivo, *J. Cell Biol. 168*, 291−302.
45. Kuo, Y. M., Emmerling, M. R., Vigo-Pelfrey, C., Kasunic, T. C., Kirkpatrick, J. B., Murdoch, G. H., Ball, M. J., and Roher, A. E. (1996) Water-soluble Abeta (N-40, N-42) oligomers in normal and Alzheimer disease brains, *J. Biol. Chem. 271*, 4077−40781.
46. Scheuner, D., Eckman, C., Jensen, M., Song, X., Citron, M., Suzuki, N., Bird, T. D., Hardy, J., Hutton, M., Kukull, W., Larson, E., Levy-Lahad, E., Viitanen, M., Peskind, E., Poorkaj, P., Schellenberg, G., Tanzi, R., Wasco, W., Lannfelt, L., Selkoe, D., and Younkin, S. (1996) Secreted amyloid beta-protein similar to that in the senile plaques of Alzheimer's disease is increased in vivo by the presenilin 1 and 2 and APP mutations linked to familial Alzheimer's disease, *Nat. Med. 2*, 864−870.
47. Amtul, Z., Lewis, P. A., Piper, S., Crook, R., Baker, M., Findlay, K., Singleton, A., Hogg, M., Younkin, L., Younkin, S. G., Hardy, J., Hutton, M., Boeve, B. F., Tang-Wai, D., and Golde, T. E. (2002) A presenilin 1 mutation associated with familial frontotemporal dementia inhibits gamma-secretase cleavage of APP and notch, *Neurobiol. Dis. 9*, 269−273.
48. Roher, A. E., Kokjohn, T. A., Esh, C., Weiss, N., Childress, J., Kalback, W., Luehrs, D. C., Lopez, J., Brune, D., Kuo, Y. M., Farlow, M., Murrell, J., Vidal, R., and Ghetti, B. (2004) The human amyloid-beta precursor protein770 mutation V717F generates peptides longer than amyloid-beta-(40−42) and flocculent amyloid aggregates, *J. Biol. Chem. 279*, 5829−5836.

BI0508237